Pergamon

Int. J. Solids Structures Vol. 35, No. 23, pp. 3007–3027, 1998

0020–7683/98 $19.00 + .00

PII: S0020–7683(97)00360–0

POSTBUCKLING OF ANISOTROPIC FLAT AND DOUBLY-CURVED SANDWICH PANELS UNDER COMPLEX LOADING CONDITIONS

TERRY HAUSE, LIVIU LIBRESCU*
Department of Engineering Science and Mechanics, Virginia Polytechnic Institute and State University, Blacksburg, VA 24061-0219, U.S.A.

and

CHARLES J. CAMARDA†
NASA Langley Research Center, Hampton, VA 23681-0001, U.S.A.

(*Received* 3 *September* 1996; *in revised form* 12 *November* 1997)

Abstract—A study of the postbuckling behavior of geometrically imperfect anisotropic sandwich doubly-curved and flat panels subjected to a system of compressive edge loads and a lateral pressure is presented. The study is carried out in the context of the weak core sandwich shell model whose superior structural performance as compared to those of the strong core sandwich or standard laminated structures has resulted in its increased use in the design of advanced flight vehicles. A detailed investigation of the influence played by a number of kinematical and physical parameters as well as by the character of tangential boundary conditions on the load carrying capacity of sandwich structures is performed and pertinent conclusions are outlined. © 1998 Elsevier Science Ltd. All rights reserved.

NOMENCLATURE

a	the distance between the global mid-surface and the mid-surface of facings
$A_{\omega\rho}$, $A^*_{\omega\rho}$	stiffness quantities associated with the facings and their inverted counterparts, respectively
$B_{\omega\rho}$, $D_{\omega\rho}$, $F_{\omega\rho}$,	stiffness quantities associated with the facings
$c_{\alpha\beta}$	2-D permutation symbol
e_{ij}	3-D strain tensor
E_1, E_2	in-plane Young's moduli
$\bar{G}_{13}$, $\bar{G}_{23}$	transverse shear moduli of the core
h, $\bar{h}$, H	thickness of the facings, that of the core and the total thickness of the structure, respectively
K	Gaussian curvature of the global mid-surface
L_1, L_2	length and width of the flat/curved panel
$L_{\alpha\beta}$, $M_{\alpha\beta}$, $N_{\alpha\beta}$	stress couples and stress resultants measures [eqns (16) and (17)]
$\bar{N}_{13}$, $\bar{N}_{23}$	transverse shear stress resultants associated with the core
$\mathcal{N}_{11}$, $\mathcal{N}_{22}$	dimensionless form of the normal edge loads
P	$\bar{q}_{mn}$, dimensionless counterpart of q_{mn} [eqn (28b)]
q_3	transverse load
$\bar{Q}_{44}$, $\bar{Q}_{55}$	transverse shear moduli associated with the core
Q_{ij}, $\bar{Q}_{ij}$	elastic moduli and their modified counterparts, respectively
r	dimensionless thickness ratio
R_1, R_2	principal radii of curvature of the global mid-surface
S_{ij}	second Piola–Kirchhoff stress tensor
V_α, V_3	3-D displacement tangential and transversal field
v_3, $\mathring{v}_3$	transversal deflection and initial geometric imperfection, respectively
x_α, x_3	tangential and the thicknesswise coordinate, respectively
δ_{mn}, $\mathring{\delta}_{mn}$	dimensionless counterparts of w_{mn} and $\mathring{w}_{mn}$, respectively
Δ_1	end-shortening in the x_1 direction
ξ_α, η_α	2-D tangential displacement measures (eqns 5)
ϕ	Airy's potential function
ε_{ij}	2-D strain measures
λ_m, μ_n	$m\pi/L_1$, $n\pi/L_2$

* Author to whom correspondence should be addressed. Tel.: 540 231 5916. Fax: 001 540 231 4574.
† Currently at NASA Johnson Space Center, Houston, TX 77058-3696.

Superscripts, subscripts and underscoring signs

$(\cdot)'$, $(\cdot)''$, $(\cdot)$	quantities affiliated with the bottom, upper and core layers, respectively
$\underline{(\cdot)}$	prescribed quantity
$\tilde{(\cdot)}_f$ $(\cdot)_c$	quantities associated with the face and core layers, respectively
$(\cdot)_{,i}$	$\partial(\cdot)/\partial x_i$
$(\cdot)_{,n}$, $(\cdot)_{,t}$	derivatives of $(\cdot)$ with respect to the coordinates normal and tangential to an edge, respectively.

1. INTRODUCTION

A typical laminated structure which, due to its outstanding features, was used in the aeronautical industry in the past and is of great promise in the design of high-speed and reusable launch vehicles, is the sandwich-type construction. In its simplest form, the sandwich construction can be viewed as a structure composed of two stiff layers (face layers), separated by a thick mid-layer of low density material (core layer). The considerable advantages offered by fibrous composite materials over conventional materials and the need of overcoming the technical challenges involving the design of advanced supersonic/hypersonic flight vehicles have prompted an increased use of sandwich structures, and incorporation in their construction of laminated composites as face sheets.

During the operational life of aerospace vehicles, high temperature and pressure gradients acting throughout their structure are likely to be experienced. As a result of these severe environmental conditions, high compressive stresses acting on the edges of the constituent panels are induced. For this reason, the study of the postbuckling behavior of sandwich structures under complex loading conditions is a matter of considerable importance in the design of supersonic/hypersonic aircraft. The results of such a study can reveal, among others, the capacity of sandwich constructions to carry compressive edge loads beyond buckling bifurcation; to support lateral pressure fields with/without the occurrence of the snap-through buckling; to infer about the severity of the snapping phenomenon and on the sensitivity of the load carrying capacity to initial geometric imperfections.

As the most actual and comprehensive survey on the status and achievements in the field of sandwich constructions reveals, (see Noor *et al.*, 1996), such results are completely lacking from the specialized literature. One of the goals of the present work is to fill this gap, by supplying pertinent information on this topic.

A basic ingredient enabling one to accomplish such a study lies on the availability of a geometrically non-linear theory of sandwich flat and curved panels incorporating the initial geometric imperfections and accounting for the anisotropy of the face sheets.

A theory of sandwich plates/shells encompassing these features and able to address such issues was recently developed (see Librescu *et al.*, 1996) and will be used for such a purpose in this paper. In order to be reasonably self-contained, in the following, the relevant equations are displayed and emphasized only to the extent that they are needed in our treatment of the subject.

2. BASIC ASSUMPTIONS

The geometrically non-linear theory of doubly curved sandwich shells used herein is based on a number of assumptions, namely: (i) the face sheets are constructed of a number of orthotropic material layers, the axes of orthotropy of the individual plies being not necessarily coincident with the geometrically axes x_α of the structure, (ii) the core material features orthotropic properties, the axes of orthotropy being parallel to the geometrically axes x_α. Although in the paper by Librescu *et al.*, 1996, the developed theory involves the cases of weak and strong core sandwich structures, here the analysis is confined to weak core sandwich structures, (iii) the core and face layers are incompressible in the transverse normal direction, (iv) although in the paper by Librescu *et al.* (1996) the theory concerns the general case of non-symmetric face sheets, herein the case of symmetric faces with respect to both the global reference surface of the panel and of those of the upper and bottom facings is considered, (v) the analysis is carried out in the framework of the shallow shell theory, and finally, (vi) a perfect bonding between the face and core layers is postulated.

3. KINEMATICS OF SANDWICH PLATES AND SHELLS

The global middle surface of the structure selected to coincide with that of the core layer, is referred to a curvilinear and orthogonal coordinate system $x_\alpha(\alpha = 1,2)$. The transverse normal coordinate x_3 is considered positive when measured in the direction of the downward normal. We also assume that the uniform thickness of the core is $2\bar{h}$ while those of the bottom and upper faces are h' and h'', respectively. As a result, $H(\equiv 2\bar{h}+h'+h'')$ is the total thickness of the structure. For the sake of identification, unless otherwise noted, the quantities affiliated with the core will be accompanied by a superposed bar, while those associated with the lower and upper faces by a single and double primes, respectively, placed on the right or left of the respective quantity. In the forthcoming developments, in addition to the global mid-surface of sandwich structure, the mid-surfaces of the upper and bottom facings will also be considered in the analysis. Their location, measured with respect to the global mid-surface, is given by $a'(\equiv \bar{h}+h'/2)$ and $a''(\equiv \bar{h}+h''/2)$.

In view of assumptions (iii) and (iv), the following relationships hold valid

$$'V_3 = ''V_3 = \bar{V}_3 \equiv v_3(x_1, x_2, t) \tag{1a}$$

and

$$h' = h'' \equiv h, \quad a' = a'' \equiv a. \tag{1b,c}$$

In eqn (1a) v_3 denotes the transversal deflection considered to be positive in the inward direction and assumed to be uniform through the entire thickness of the structure. In the dynamic case, the time-dependence of the field quantities has to be accounted for. Upon representing the tangential 3-D displacements corresponding to the face and core layers in a linear form throughout their thickness, discarding transverse shear effects in the face sheets, taking into account eqn (1a) and enforcing the kinematic continuity conditions at the interfaces between the core and facings, one obtains their expressions given by:

$$\left.\begin{aligned} 'V_1(x_\alpha, x_3) &= \xi_1(x_\alpha)+\eta_1(x_\alpha)-(x_3-a)\frac{\partial v_3(x_\alpha)}{\partial x_1} \\ 'V_2(x_\alpha, x_3) &= \xi_2(x_\alpha)+\eta_2(x_\alpha)-(x_3-a)\frac{\partial v_3(x_\alpha)}{\partial x_2} \\ 'V_3(x_\alpha, x_3) &= v_3(x_\alpha) \end{aligned}\right\} \bar{h} \leqslant x_3 \leqslant \bar{h}+h \tag{2a–c}$$

$$\left.\begin{aligned} \bar{V}_1(x_\alpha, x_3) &= \xi_1(x_\alpha)+(x_3/\bar{h})\left\{\eta_1(x_\alpha)+\frac{h}{2}\frac{\partial v_3(x_\alpha)}{\partial x_2}\right\} \\ \bar{V}_2(x_\alpha, x_3) &= \xi_2(x_\alpha)+x_3/\bar{h}\left\{\eta_2(x_\alpha)+\frac{h}{2}\frac{\partial v_3(x_\alpha)}{\partial x_2}\right\} \\ \bar{V}_3(x_\alpha, x_3) &= v_3(x_\alpha) \end{aligned}\right\} -\bar{h} \leqslant x_3 \leqslant \bar{h} \tag{3a–c}$$

$$\left.\begin{aligned} ''V_1(x_\alpha, x_3) &= \xi_1(x_\alpha)-\eta_1(x_\alpha)-(x_3+a)\frac{\partial v_3(x_2)}{\partial x_1} \\ ''V_2(x_\alpha, x_3) &= \xi_2(x_2)-\eta_2(x_\alpha)-(x_3+a)\frac{\partial v_3(x_\alpha)}{\partial x_2} \\ ''V_3(x_\alpha, x_3) &= v_3(x_\alpha) \end{aligned}\right\} -\bar{h}-h'' \leqslant x_3 \leqslant \bar{h}. \tag{4a–c}$$

A detailed deduction of eqns (2)–(4) can be found in the paper by Librescu *et al.* (1996). In these equations $\xi_1(x_1, x_2)$, $\xi_2(x_1, x_2)$, $\eta_1(x_1, x_2)$ and $\eta_2(x_1, x_2)$ stand for the 2-D tangential displacement measures defined as

$$\xi_1 = ('V_1^0 + ''V_1^0)/2, \quad \eta_1 = ('V_1^0 - ''V_1^0)/2,$$
$$\xi_2 = ('V_1^0 + ''V_2^0)/2, \quad \eta_2 = ('V_2^0 - ''V_2^0)/2, \tag{5a–d}$$

where $'V_\alpha^0$, and $''V_\alpha^0$ denote the tangential displacements of the points of the mid-surface of the bottom and upper face sheets, respectively.

In light of eqns (2)–(4) it is readily seen that the 3-D displacement field of sandwich shells is expressible in terms of the 2-D displacement measures ξ_1, ξ_2, η_1, η_2 and v_3. Assuming that the structure features also a stress-free initial geometric imperfection $\mathring{V}_3(\equiv \mathring{v}_3(x_\alpha))$, and adopting the concept of small strains and moderately small rotations (see Librescu, 1987), the 3-D Lagrangian strain tensor, e_{ij}, produced by a field of finite displacements V_i is given by

$$2e_{ij} = V_{i\|j} + V_{j\|i} + V_{3\|i}V_{3\|j} + V_{3\|i}\mathring{V}_{3\|j} + \mathring{V}_{3\|i}V_{3\|j}. \tag{6}$$

By convention, the transverse deflection is measured from the imperfect surface, in the positive, inward direction. In eqn (6) $(\cdot)_{i\|j}$ denotes the covariant derivative with respect to the metric of the 3-D space. Using the relationships between covariant derivatives of space and surface tensors, (see Librescu, 1975), from eqns (2)–(6) and consistent with the concept of shallow shells, the distribution of strain quantities across the laminate thickness assumes the form:

In the bottom facing: $(\bar{h} \leqslant x_3 \leqslant \bar{h} + h')$

$$'e_{11} = '\varepsilon_{11} + (x_3 - a')\kappa'_{11}, \quad 'e_{22} = '\varepsilon_{22} + (x_3 - a')\kappa'_{22}, \quad 2'e_{12} = '\gamma_{12} + (x_3 - a')\kappa'_{12}. \tag{7a–c}$$

In the core layer: $(-\bar{h} \leqslant x_3 \leqslant \bar{h})$

$$\bar{e}_{11} = \bar{\varepsilon}_{11} + x_3\bar{\kappa}_{11}, \quad \bar{e}_{22} = \bar{\varepsilon}_{22} + x_3\bar{\kappa}_{22}, \quad 2\bar{e}_{12} = \bar{\gamma}_{12} + x_3\bar{\kappa}_{12}, \quad 2\bar{e}_{13} = \bar{\gamma}_{13}, \quad 2\bar{e}_{23} = \bar{\gamma}_{23} \tag{8a–e}$$

and

In the upper facing: $(-\bar{h} - h'' \leqslant x_3 \leqslant -\bar{h})$

$$''e_{11} = ''\varepsilon_{11} + (x_3 + a'')\kappa''_{11}, \quad ''e_{22} = ''\varepsilon_{22} + (x_3 + a'')\kappa''_{22}, \quad 2''e_{12} = ''\gamma_{12} + (x_3 + a'')\kappa''_{12}. \tag{9a–c}$$

In these equations ε_{11}, ε_{22}, $\varepsilon_{12}(\equiv\gamma_{12}/2)$ and $\varepsilon_{13}(\equiv\gamma_{13}/2)$, $\varepsilon_{23}(\equiv\gamma_{23}/2)$ denote the 2-D tangential and the transverse shear strain measures, respectively. Their expressions in terms of the 2-D displacement measures are displayed in Appendix 1.

4. EQUATIONS OF EQUILIBRIUM/MOTION AND BOUNDARY CONDITIONS

The Hamilton's variational principle is used to derive the equations of equilibrium/motion and the boundary conditions of the theory of shallow sandwich shells. This variational principle may be stated as

$$\delta J = \delta \int_{t_0}^{t_1} (U - W - T)\,\mathrm{d}t = 0 \tag{10}$$

where t_0, t_1 are two arbitrary instants of time; U denotes the strain energy; W denotes the work done by surface tractions, transversal, edge loads and body forces; T the kinetic energy of the 3-D body of the sandwich structure, while δ denotes the variational operator.

The variations of the strain energy, of the kinetic energy and of the work are given, respectively, by

$$\delta U = \frac{1}{2}\int_\sigma \left[\int_{\bar h}^{\bar h + h'} {}' S_{ij}\delta e'_{ij} + \int_{\bar h}^{+h'} \bar S_{ij}\delta \bar e_{ij} + \int_{-\bar h - h''}^{-\bar h} {}'' S_{ij}\delta e''_{ij}\right] \mathrm{d}x_3\,\mathrm{d}\sigma, \quad (i,j = 1,2,3) \tag{11}$$

$$\int_{t_0}^{t_1} \delta T\,\mathrm{d}t = -\int_{t_0}^{t_1} \mathrm{d}t\left[\int_\sigma \int_{\bar h}^{\bar h + h'} {}' \rho \ddot V_i \delta V_i\,\mathrm{d}x_3 \int_{-\bar h}^{\bar h} \bar\rho \ddot V_i \delta V_i\,\mathrm{d}x_3 + \int_{-\bar h - h''}^{-\bar h} {}'' \rho \ddot V_i \delta V_i\,\mathrm{d}x_3\right], \tag{12}$$

where it was considered that $\delta V_i = 0$ at $t = t_0, t_1$, while

$$\delta W = \int_\sigma \left[\int_{\bar h}^{\bar h + h'} {}' \rho H_i \delta V_i\,\mathrm{d}\sigma\,\mathrm{d}x_3 + \int_{-\bar h}^{\bar h} \bar\rho H_i \delta V_i\,\mathrm{d}\sigma\,\mathrm{d}x_3 + \int_{-\bar h - h''}^{-\bar h} {}'' \rho H_i \delta V_i\,\mathrm{d}\sigma\,\mathrm{d}x_3\right] + \int_{\Omega_s} \underset{\sim}{S}_i \delta V_i\,\mathrm{d}\Omega. \tag{13}$$

Herein, the usual summation convention over a repeated index is employed; S_{ij} denotes the second Piola–Kirchhoff stress tensor, σ denotes the undeformed mid-surface of the sandwich shell, the superposed dots denote time derivatives, ρ denotes the mass density; $\underset{\sim}{S}_i = \underset{\sim}{S}_{ij} n_j$ denote the components of the stress vector prescribed on the part Ω_s of the external boundary Ω; n_i are the components of the outward unit vector normal to Ω and H_i denote the components of the body force vector.

From the variational eqn (10) considered in conjunction with eqns (11)–(13), and with the strain–displacement relationships (7)–(9) (used as subsidiary conditions), carrying out the integration with respect to x_3 and integrating by parts wherever feasible, using the definition of global stress resultants and stress couples (to be defined later), and invoking the arbitrary and independent character of variations $\delta\xi_1$, $\delta\xi_2$, $\delta\eta_1$, $\delta\eta_2$, and δv_3 throughout the 3-D body and within the time interval $[t_0, t_1]$, one derives the equations of equilibrium/motion and the boundary conditions. By retaining only the transversal load and transverse inertia term, the equations of motion are:

$$\begin{aligned}
&\delta\xi_1: \quad N_{11,1} + N_{12,2} = 0,\\
&\delta\xi_2: \quad N_{22,2} + N_{12,1} = 0,\\
&\delta\eta_1: \quad L_{11,1} + L_{12,2} - \bar N_{13} = 0,\\
&\delta\eta_2: \quad L_{22,2} + L_{12,1} - \bar N_{23} = 0,\\
&\delta v_3: \quad N_{11}(v_{3,11} + \mathring v_{3,11} + 1/R_1) + 2N_{12}(v_{3,12} + \mathring v_{3,12}) + N_{22}(v_{3,22}\mathring v_{3,22} + 1/R_2)\\
&\qquad + (M_{11,11} + 2M_{12,12} + M_{22,22})(1 + h/2\bar h)(\bar N_{13,1} + \bar N_{23,2}) + q_3 - m_0 \ddot v_3 = 0.
\end{aligned} \tag{14a–e}$$

As concerns the associated boundary conditions, these are:

$$\begin{aligned}
&N_{nn} = \underset{\sim}{N}_{nn}, && \text{or} \quad \xi_n = \underset{\sim}{\xi}_n,\\
&N_{nt} = \underset{\sim}{N}_{nt}, && \text{or} \quad \xi_t = \underset{\sim}{\xi}_t,\\
&L_{nn} = \underset{\sim}{L}_{nn}, && \text{or} \quad \eta_n = \underset{\sim}{\eta}_n,\\
&L_{nt} = \underset{\sim}{L}_{nt}, && \text{or} \quad \eta_t = \underset{\sim}{\eta}_t,\\
&M_{nn} = \underset{\sim}{M}_{nn}, && \text{or} \quad v_{3,n} = \underset{\sim}{v}_{3,n},\\
&N_{nt}(v_{3,t} + \mathring v_{3,t}) + N_{nn}(v_{3,n} + \mathring v_{3,n}) + M_{nn,n}, && \text{or} \quad v_3 = \underset{\sim}{v}_3.\\
&\quad + 2M_{nt,t} + (1 + h/2(2\bar h))\bar N_{n3} = \underset{\sim}{M}_{nt,t} \pm \bar N_{n3}.
\end{aligned} \tag{15a–f}$$

In these equations $1/R_1$ and $1/R_2$ denote the principal curvatures of the global middle surface in the reference configuration; $(\,)_{,\alpha}$ denotes the partial differentiation with respect

to surface coordinates x_α, while q_3 and m_0 denote the distributed transversal load and the reduced mass per unit area of the shell mid-surface repeated. The subscripts n and t in eqns (15) are used to designate the normal and tangential in-plane directions to an edge, and hence $n = 1$ when $t = 2$, and vice-versa. The terms underscored by a tilde denote prescribed quantities. As concerns the global stress resultants and stress couples in terms of which eqns (14) and (15) are expressed, for weak core sandwich structures these reduce to:

$$
\begin{aligned}
N_{11} &= {}'N_{11} + {}''N_{11}, \quad (1 \rightleftarrows 2) \\
N_{12} &= {}'N_{12} + {}''N_{12}, \\
L_{11} &= \bar{h}({}'N_{11} - {}''N_{11}), \quad (1 \rightleftarrows 2) \\
L_{12} &= \bar{h}({}'N_{12} - {}''N_{12}), \\
M_{11} &= {}'M_{11} + {}''M_{11}, \quad (1 \rightleftarrows 2) \\
M_{12} &= {}'M_{12} + {}''M_{12}.
\end{aligned} \tag{16a–f}
$$

The sign $(1 \rightleftarrows 2)$ indicates that the expressions of the stress resultants and stress couples not explicitly written can be obtained from the ones associated with this sign upon replacing subscript 1 by 2 and vice versa.

Consistent with the concept of shallow shell theory, the stress resultants and stress couples in the bottom facings are expressed as:

$$
\{N'_{\alpha\beta}, M'_{\alpha\beta}\} = \sum_{k=1}^{N} \int_{(x_3)_{k-1}}^{(x_3)_k} {}'(S_{\alpha\beta})_k \{1, x_3 - a\} \, \mathrm{d}x_3, \quad (\alpha, \beta = 1, 2) \tag{17}
$$

and in the core layer as:

$$
\bar{N}_{\alpha 3} = \int_{-\bar{h}}^{\bar{h}} \bar{S}_{\alpha 3} \, \mathrm{d}x_3. \tag{18}
$$

The stress resultants and stress couples for the upper facings can be formally obtained from those defined by eqns (17) by replacing single primes by double primes and a by $-a$. Herein N denotes the number of constituent layers in the bottom facings (which, by virtue of the postulated symmetry is equal with that in the upper facings), while $(x_3)_k$ and $(x_3)_{k-1}$ denote the distances from the global reference surface (coinciding with that of the core layer) the upper and bottom interfaces of the kth layer, respectively. It should be recalled that eqns (14)–(16) corresponding to weak core sandwich structures represent the specialized counterpart of the more general ones derived in the paper by Librescu *et al.* (1996).

5. CONSTITUTIVE EQUATIONS

Assuming a symmetric lay-up for the faces and that the material of the constituent layers feature monoclinic symmetry properties, in the absence of thermal and moisture effects, the constitutive equations associated with the bottom facings assume the form (see Librescu *et al.* (1996)):

$$
\begin{aligned}
{}'N_{11} &= A'_{11}\varepsilon'_{11} + A'_{12}\varepsilon'_{22} + A'_{16}\gamma'_{12}, \quad (1 \rightleftarrows 2) \\
{}'N_{12} &= A'_{16}\varepsilon'_{11} + A'_{26}\varepsilon'_{22} + A'_{66}\gamma'_{12}, \\
{}'M_{11} &= F'_{11}\kappa'_{11} + F'_{12}\kappa'_{22} + F'_{16}\gamma'_{12}, \quad (1 \rightleftarrows 2) \\
{}'M_{12} &= F'_{16}\kappa'_{11} + F'_{26}\kappa'_{22} + F'_{66}\gamma'_{12}.
\end{aligned} \tag{19a–d}
$$

The stiffness quantities in eqns (18) are defined as

$$F'_{\omega\rho} = D'_{\omega\rho} - 2aB'_{\omega\rho} - a^2 A'_{\omega\rho} \tag{20a}$$

and

$$\{A'_{\omega\rho}, B'_{\omega\rho}, D'_{\omega\rho}\} = \sum_{k=1}^{N'} \int_{(x_3)_{k-1}}^{(x_3)_k} (\hat{Q}'_{\omega\rho})_{(k)}(1, x_3, x_3^2)\, \mathrm{d}x_3, \quad (\omega, \rho = 1, 2, 6). \tag{20b}$$

The expression of stress resultants and stress couples associated with the upper facings can be obtained formally from eqns (19) and (20) by replacing the single prime by double primes and a by $-a$. However, in view of the symmetry with respect to the global mid-surface, $N' = N''$ and by virtue of the overall symmetry of the structure with respect to the global mid-surface, one has in addition $\hat{Q}'_{\omega\rho} = \hat{Q}''_{\omega\rho}$.

For the core layer considered as an orthotropic body (the axes of orthotropy coinciding with the geometrical axes), upon postulating that it is capable of carrying only transverse shear stresses, the pertinent constitutive equations reduce to:

$$\bar{N}_{13} = 2\bar{h}\bar{K}^2\bar{Q}_{55}\bar{\gamma}_{13}, \quad \bar{N}_{23} = 2\bar{h}\bar{K}^2\bar{Q}_{44}\bar{\gamma}_{23}. \tag{21a,b}$$

In eqn (20b) the reduced elastic moduli $\hat{Q}_{ij}$ are defined as $\hat{Q}_{ij} = Q_{ij} - (Q_{i3}Q_{j3})/Q_{33}$, while in eqns (21) $\bar{K}^2$ defines the transverse shear correction factor.

6. GOVERNING EQUATIONS

A representation of governing equations most suitable for buckling and postbuckling studies will be used. This representation can be seen as a generalization for the case of sandwich shells of that used in the case of shear deformable shallow shell theory (see Librescu and Chang, 1992; Librescu *et al.*, 1993), as well as of that for flat sandwich structures (see Librescu, 1975). For the case considered here the representation is done in terms of the Airy's potential function $\phi(x_1, x_2)$, the transverse displacement v_3 and the displacements measures η_1 and η_2.

To this end the equilibrium eqns (14a, b) are identically fulfilled by expressing the stress resultants in terms of the Airy's potential function $\phi(\equiv \phi(x_\omega))$ as:

$$N_{\alpha\beta} = c_{\alpha\omega}c_{\beta\rho}\phi_{,\omega\rho} \tag{22}$$

where $c_{\alpha\beta}$ denotes the 2-D permutation symbol. Having in view that with the use of eqn (22), the two equilibrium equations are eliminated, in order to ensure single valued displacements, the compatibility equation for the tangential strain measures has to be fulfilled.

For weak core doubly curved sandwich panels this equation is:

$$\varepsilon_{11,22} + \varepsilon_{22,11} - \gamma_{12,2} + (2/R_1)v_{3,22} + (2/R_2)v_{3,11} - 2v_{3,12}^2 + 2v_{3,11},v_{3,22} + 2\mathring{v}_{3,11}v_{3,22} - 4v_{3,12}\mathring{v}_{3,22} = 0 \tag{23}$$

where

$$\varepsilon_{11} = {}'\varepsilon_{11} + {}''\varepsilon_{11}; \quad \varepsilon_{22} = {}'\varepsilon_{22} + {}''\varepsilon_{22}; \quad \gamma_{12} = {}'\gamma_{12} + {}''\gamma_{12}.$$

Equation (23) can be expressed in terms of the basic functions mentioned above by performing a partial inversion of eqns (19a, b). Having in view these equations considered in conjunction with eqn (22), the compatibility equation can now be expressed as:

$$A^*_{22}\phi_{,1111}+A^*_{11}\phi_{,2222}-2A^*_{16}\phi_{,1222}-2A^*_{26}\phi_{,2111}+(A^*_{66}+2A^*_{12})\phi_{,1122}+(2/R_1)v_{3,22}$$
$$+(2/R_2)v_{3,11}-2v^2_{3,12}+2v_{3,11}v_{3,22}+2\mathring{v}_{3,11}v_{3,22}+2v_{3,11}\mathring{v}_{3,22}-4v_{3,12}\mathring{v}_{3,12}=0. \quad (24)$$

By virtue of the structural symmetry of the sandwich panel, in these equations,

$$A_{\alpha\beta}\equiv(A'_{\alpha\beta}=A''_{\alpha\beta}),\quad F_{\alpha\beta}\equiv(F'_{\alpha\beta}=F''_{\alpha\beta}),\quad h\equiv(h'=h''),$$

whereas the stiffness quantities $A^*_{\alpha\beta}$ represent the inverted counterparts of $A_{\alpha\beta}$.

On the other hand, the equilibrium equation (14c–e) expressed in terms of the displacement quantities write:

$$A_{11}\eta_{1,11}+A_{16}\eta_{2,11}+A_{66}\eta_{1,22}+(A_{12}+A_{66})\eta_{2,12}+2A_{16}\eta_{1,12}+A_{26}\eta_{2,22}$$
$$-(2\bar{K}^2\bar{G}_{13}/\bar{h})(\eta_1+av_{3,1})=0, \quad (25a)$$

$$A_{22}\eta_{2,22}+A_{26}\eta_{1,22}+A_{66}\eta_{2,11}+(A_{12}+A_{66})\eta_{1,12}+2A_{26}\eta_{2,12}+A_{16}\eta_{1,11}$$
$$-(2\bar{K}^2\bar{G}_{23}/\bar{h})(\eta_2+av_{3,2})=0, \quad (25b)$$

$$\phi_{,22}(v_{3,11}+\mathring{v}_{3,11}+1/R_1)+\phi_{,11}(v_{3,22}+\mathring{v}_{3,22}+1/R_2)-2\phi_{,12}(v_{3,12}+\mathring{v}_{3,12})$$
$$-F_{11}v_{3,1111}-F_{22}v_{3,2222}-4F_{16}v_{3,1112}-4F_{26}v_{3,1222}-2(F_{12}+2F_{66})v_{3,1122}$$
$$+(2\bar{K}^2a/\bar{h})\{\bar{G}_{13}(\eta_{1,1}+av_{3,11})+\bar{G}_{23}(\eta_{2,2}+av_{3,22})\}-m_0\ddot{v}_3+q_3=0. \quad (25c)$$

Equations (24) and (25) constitute the governing equations of the problem. The analysis will be confined to simply-supported boundary conditions. Since for geometrically nonlinear problems, the bending and stretching problems are coupled, in addition to the bending boundary conditions, the ones associated with the tangential boundary conditions have also to be fulfilled. The formulation of the latter ones gives rise to two types of tangential boundary condition, referred to herein as movable and immovable edge conditions (see e.g. Librescu *et al.*, 1995). These correspond to the case when the motion of the unloaded edges in the plane tangent to the structure's mid-surface, normal to the respective edge is either unrestrained or completely restrained, respectively. As a result, we have:

Case (I). Edges $x_n=$ const., are loaded in compression and freely movable. In this case, along these edges the following conditions have to be fulfilled:

$$N_{nn}=-\underset{\sim}{N}_{nn},\quad N_{nt}=0,\quad \eta_n=0,\quad \eta_t=0,\quad M_{nn}=0,\quad v_3=0. \quad (26a\text{–}f)$$

Case (II). Edges $x_n=$ const. are unloaded and immovable. In this case

$$\xi_n=0,\quad N_{nt}=0,\quad \eta_n=0,\quad \eta_t=0,\quad M_{nn}=0,\quad v_3=0. \quad (27a\text{–}f)$$

As previously, n and t designate the normal and tangential in-plane directions to an edge, respectively.

The condition expressing the immovability conditions $\xi_n=0$ on $x_n=$ const. is fulfilled in an average sense as $\int_0^{L_t}\int_0^{L_n}(\partial\xi_n/\partial x_n)\,dx_n\,dx_t=0$. This condition in conjunction with the expressions of $'\varepsilon_{11}$ and $''\varepsilon_{11}$ from the Appendix 1 provides the fictitious edge load $\underset{\sim}{N}_{nn}$ rendering the edges $x_n=$ const., immovable. When all edges are immovable, the above condition has to be applied to both pairs of opposite edges as to determine the pertinent fictitious edge loads $\underset{\sim}{N}_{11}$ and $\underset{\sim}{N}_{22}$.

7. POSTBUCKLING ANALYSIS

In order to assess the influence played by a number of non-classical effects, the case of the cross-ply laminated facings is considered, this implying $A_{16}=A_{26}=0$ and $F_{16}=F_{26}=0$. The expression of transverse deflection satisfying the boundary condition $v_3=0$ is

$$v_3(x_1, x_2) = w_{mn} \sin \lambda_m x_1 \sin \mu_n x_2 \tag{28a}$$

and the transversal load is represented as

$$q_3(x_1, x_2) = q_{mn} \sin \lambda_m x_1 \sin \mu_m x_2 \tag{28b}$$

where $\lambda_m = m\pi/L_1$, and $\mu_n = n\pi/L_2$, L_1 and L_2 being the panel side edge dimensions while w_{mn} are the modal amplitudes. Following the results by Seide (1974) and Simitses (1986), the representation of initial geometric imperfections resulting, for the problem at hand, in the most critical postbuckling conditions is

$$\mathring{v}_3(x_1, x_2) = \mathring{w}_{mn} \sin \lambda_m x_1 \sin \mu_n x_2, \tag{29}$$

where $\mathring{w}_{mn}$ are the modal amplitudes of the initial geometric imperfection shape. Moreover, the stress function ϕ is expressed as (see Librescu, 1975; Librescu and Chang, 1992; Librescu 1965)

$$\phi(x_1) = \phi_1(x_2) - \tfrac{1}{2}(\underset{\sim}{N}_{11} x_2^2 + \underset{\sim}{N}_{22} x_1^2 - 2\underset{\sim}{N}_{12} x_1 x_2), \tag{30}$$

where, $\underset{\sim}{N}_{11}$, $\underset{\sim}{N}_{22}$ and $\underset{\sim}{N}_{12}$ represent the average compressive and shear edge loads while ϕ_1 is a particular solution of eqn (24). Replacement of eqns (28)–(30) into eqn (24), and solving the resulting non-homogeneous partial differentiation equation, along the lines described in the papers by Librescu (1995) and Librescu and Chang (1993), yields the expression of ϕ_1 as:

$$\phi_1(x_\alpha) = A_1 \cos 2\lambda_m x_1 + A_2 \cos 2\mu_n x_2 + A_3 \sin \lambda_m x_1 \sin \mu_n x_2 \tag{31}$$

where its coefficients are obtained as:

$$A_\alpha = \tilde{A}_\alpha (w_{mn}^2 + 2 w_{mn} w_{mn}^0), \quad A_3 = \tilde{A}_3 w_{mn} \quad (\alpha = 1, 2). \tag{32}$$

The constants $\tilde{A}_\alpha$, $\tilde{A}_3$ are displayed in the Appendix 2.

It can readily be seen that the particular solution ϕ_1 satisfies the conditions:

$$\int_0^{L_2} \phi_{1,22}|_{x_1 = 0, L_1} \, dx_2 = 0, \quad \int_0^{L_1} \phi_{1,11}|_{x_2 = 0, L_2} \, dx_1 = 0,$$

$$\int_0^{L_2} \phi_{1,12}|_{x_1 = 0, L_1} \, dx_2 = 0, \quad \int_0^{L_1} \phi_{1,12}|_{x_2 = 0, L_2} \, dx_1 = 0,$$

$$\int_0^{L_2} \phi_{1,22}|_{x_1 = 0, L_1} \, dx_2 = -\underset{\sim}{N}_{11} L_2,$$

$$\int_0^{L_1} \phi_{1,11}|_{x_2 = 0, L_2} \, dx_1 = -\underset{\sim}{N}_{22} L_1. \tag{33a–f}$$

Equations (33) reveal that as a result of the representation eqn (30), $\underset{\sim}{N}_{11}$ and $\underset{\sim}{N}_{22}$ acquire the meaning of average in-plane compressive edge loads.

As in the case of eqn (24) by using eqn (28a), the coupled eqns (25a, b) can now be satisfied by assuming $\eta_1(x_1, x_2)$ and $\eta_2(x_1, x_2)$ in the form

$$\eta_1(x_\omega) = B_1 \cos \lambda_m x_1 \sin \mu_n x_2, \quad \eta_2(x_\omega) = C_1 \sin \lambda_m x_1 \cos \mu_n x_2 \tag{34a,b}$$

where the coefficients B_1 and C_1 can be expressed as:

$$B_1 = \tilde{B}_1 w_{mn}, \quad C_1 = \tilde{C}_1 w_{mn}.$$

The coefficients $\tilde{B}_1$ and $\tilde{C}_1$ are displayed in the Appendix 2.

Next, $\xi_1(x_1, x_2)$ and $\xi_2(x_1, x_2)$ have to be determined. To this end one uses the equations

$$N_{11} = \phi_{,22} = A_{11}\xi_{1,1} + A_{12}\xi_{2,2} + A_{11}v_{3,1}^2/2 + A_{11}\mathring{v}_{3,1}v_{3,1} - A_{11}(v_3/R_1) + A_{12}v_{3,2}^2/2 + A_{12}\mathring{v}_{3,2}v_{3,2} - A_{12}(v_3/R_2) \quad (1 \rightleftarrows 2) \tag{35a}$$

$$N_{12} = -\phi_{,12} = A_{66}\xi_{1,2} + A_{66}\xi_{1,2} + A_{66}\mathring{v}_{3,1}v_{3,2} - A_{66}v_{3,1}\mathring{v}_{3,2} + A_{66}v_{3,1}v_{3,2}. \tag{35b}$$

From eqns (25) considered in conjunction with eqns (28) and (31) one can determine ξ_1 and ξ_2 as:

$$\xi_1(x_1, x_2) = D_1 x_1 + D_2 \sin 2\lambda_m x_1 + D_3 \sin 2\lambda_m x_1 \cos 2\mu_n x_2 + D_4 \cos \lambda_m x_1 \sin \mu_n x_2 + (D_5 \underset{\sim}{N}_{11} + D_6 \underset{\sim}{N}_{22})x_1 \tag{36a}$$

$$\xi_2(x_1, x_2) = E_1 x_2 + E_2 \sin 2\mu_n x_2 + E_3 \cos 2\lambda_u x_1 \sin 2\mu_n x_2 + (E_4 \sin \lambda_m x_1 \cos \mu x_2) + (E_5 \underset{\sim}{N}_{11} + E_6 \underset{\sim}{N}_{22})x_2. \tag{36b}$$

Herein $(D_i, E_i) = (\tilde{D}_i, \tilde{E}_i)(w_{mn}^2 + 2w_{mn}\mathring{w}_{mn})$, $D_4 = \tilde{D}_4 w_{mn}$, $E_4 = \tilde{E}_4 w_{mn} (i = 1, 2, 3)$ where the expressions of $\tilde{D}_i$, $\tilde{E}_i (i = \overline{1,4})$ and of D_5, D_6, E_5 and E_6 are provided in the Appendix 2.

One of the methods enabling one to get the postbuckling equations in terms of the modal amplitudes consists of the discretization of eqn (25c) via the Galerkin method (see e.g. Librescu, 1975; Librescu and Chang, 1992; Librescu *et al.* 1993). However, a more inclusive way permitting among others, to compensate the non-fulfilment of certain boundary conditions (namely of non-essential ones) rests on the use of the extended Galerkins' method (see Fulton, 1961). To this end, replacement of the expressions of ϕ, v_3, $\mathring{v}_3$, η_1, η_2, ξ_1 and ξ_2 into the variational equation, eqn (10), and carrying out the indicated integrations, results in the following nonlinear algebraic equation expressed in terms of the modal amplitudes $\delta_{mn} (\equiv w_{mn}/H)$ as:

$$P_1[\delta_{mn}, \mathring{\delta}_{mn}, \mathscr{N}_{11}, \mathscr{N}_{22}] + P_2[\delta_{mn}^2, \delta_{mn}, \mathring{\delta}_{mn}] + P_3[\delta_{mn}^3, \delta_{mn}^2, \delta_{mn}, \mathring{\delta}_{mn}] + P_{mn}\left(\frac{\mathscr{N}_{22}}{R_2} + \frac{\mathscr{N}_1}{R_1}\right) + \tilde{q}_{mn} = 0, \quad \begin{pmatrix} m = 1, \ldots, M \\ n = 1, \ldots, N \end{pmatrix}. \tag{37}$$

In these equations P_1, P_2 and P_3 are linear, quadratic and cubic polynomials of the unknown modal amplitudes, P_{mn} are constants that depend on the material and geometric properties of the shell, $\mathscr{N}_{11}$ and $\mathscr{N}_{22}$ are normalized forms of normal edge loads to be defined later, $\mathring{\delta}_{mn} (\equiv \mathring{w}_{mn}/H)$ denote the modal imperfection amplitudes while $\tilde{q}_{mn}$ is the normalized expression of the lateral load amplitudes.

The equilibrium configurations for a given flat or curved panel are determined by solving the nonlinear algebraic eqns (37) via Newton's method. As a by-product, the values of $\mathscr{N}_{11}$ and $\mathscr{N}_{22}$ fulfilling the linearized counterpart of eqn (37) corresponding to $\delta_{mn} \neq 0$ can be obtained. These correspond to the buckling bifurcation solution. In the following, a number of numerical illustrations related to the buckling and postbuckling behavior are displayed.

8. NUMERICAL ILLUSTRATIONS

In order to provide an assessment of the linearized portion of the obtained governing equations, results on buckling response predicted by the present structural model are compared with their experimental counterparts (see Karavanov, 1960), obtained for the case of a circular cylindrical sandwich panel. The experimental data have been obtained

Table 1. Comparisons of theoretical and experimental buckling predictions for a cylindrical sandwich panel with isotropic facings of duraluminum, $\nu = 0.3$, $E = 6.96 \times 10^5$ kg/cm^2 and transversely isotropic core (of penoplast)

Case	$\bar{h}$ (cm)	$\bar{G}$ (kg/cm^2)	$(N_{11})_{cr}$	$\bar{N}_{11}L_2 \times 10^3$ kg		
				Theory	Exp	% Error
1	0.750	81.3	0.365	9.114	8.2	+11.4
2	0.750	84	0.373	9.3	7.8	+19.23
3	0.475	150	0.977	10.49	8.9	+17.865
4	0.200	127	2.726	6.643	6.28	+5.78
5	0.200	566	6.708	16.35	14.6	+11.99
6	0.225	92	2.023	5.965	5.0	+19.3
7	0.500	32.6	0.431	5.087	4.4	+15.61
8	0.475	40	0.5	5.369	4.62	+16.212
9	0.500	141	0.879	10.36	9.25	+12.00
10	0.700	104	0.468	10.26	8.55	+20.00

for a panel having the geometrical characteristics $L_1 = 60$ cm, $L_2 = 40$ cm, $R_2(\equiv R) = 100$ cm, $h = 0.1$ cm.

The theoretical predictions displayed in Table 1 reveal overpredictions of the experimental ones in the range of (5–20%).

Consideration of initial geometric imperfections and of other uncertainties affecting the test specimens would have eliminated this disparity of results. In fact, the knockdown factor which is still considered a useful tool for successful shell design (see e.g. Bushnell, 1985; Arbocz, 1997), is used to reduce the theoretical buckling predictions (obtained within the assumption of the geometrically perfect shell model) to the experimental ones. As the results reveal, for the present case, such a knockdown factor should be no greater than 20%, whereas in the usual cases this factor may be much larger.

In this light it should be concluded that the two groups of results displayed in Table 1 are less far apart than expected.

As concerns the non-linear response, two types of three-layer sandwich structures are considered in the numerical illustrations, namely: Type (i) characterized by isotropic facings and transversely-isotropic core, and Type (ii) in which both the facings and the core are orthotropic. For these cases, the elastic and geometric parameters are appropriately selected as:

$$\text{Type (i)}: \quad E_f/G_c = 50; \quad \nu = 0.3; \quad h/L = 0.002; \quad h_c/L = 0.03$$

$$\text{Type (ii)}: \quad (G_{12}/E_2)_f = 0.6; \quad (E_2)_f/(G_{13})_c = 10;$$

$$(G_{13}/G_{23})_c = 2.5; \quad h/L = 0.002; \quad h_c/L = 0.03.$$

In the following, the non-specification of the type of structure implies its belonging to the Type (i). It should be noticed that in both types of structures, the same thickness characteristics have been considered.

For the problem at hand it is convenient to identify the quantities affiliated with the face and core layers by associating to these ones the indices f and c, respectively.

The parameters $(\mathcal{N}_{11}, \mathcal{N}_{22}) = (rn^2/(\mu_n^2 F_{22})(\mathcal{N}_{11}, \mathcal{N}_{22})$ and $P = \tilde{q}_{mn}(\equiv (q_{mn} r L_2^4)/(\pi^2 F_{22} H))$ where $r(\equiv \{h/[\sqrt{3}(2h_c + h)]\}^2$ defines the thickness ratio. In addition, the quantity $\Delta_1(\equiv -(1/L_1 L_2)\int_0^{L_1}\int_0^{L_2}(\partial\xi_1/\partial x_1)\,dx_1\,dx_2)$ defines the end shortening in the x_1-direction.

For the sake of simplicity one considers the case of curved panels featuring a square projection on a plane, this implying that $L_1 = L_2 \equiv L$. In this case, the most conservative buckling/postbuckling conditions occur for $m = n = 1$. Consequently, $\delta(\equiv w_{11}/H)$ and $\delta_0(\equiv w_{11}^0/H)$ stand for the deflection and imperfection amplitudes obtained at the center of the panel, $x_1 = x_2 = L/2$. The effects of a lateral pressure on the deflection of doubly curved panels are depicted in Figs 1–3.

In Fig. 1 the case of a geometrically spherical cape with movable edges is considered while in Figs 2 and 3 the response to a lateral pressure of doubly-curved panels featuring

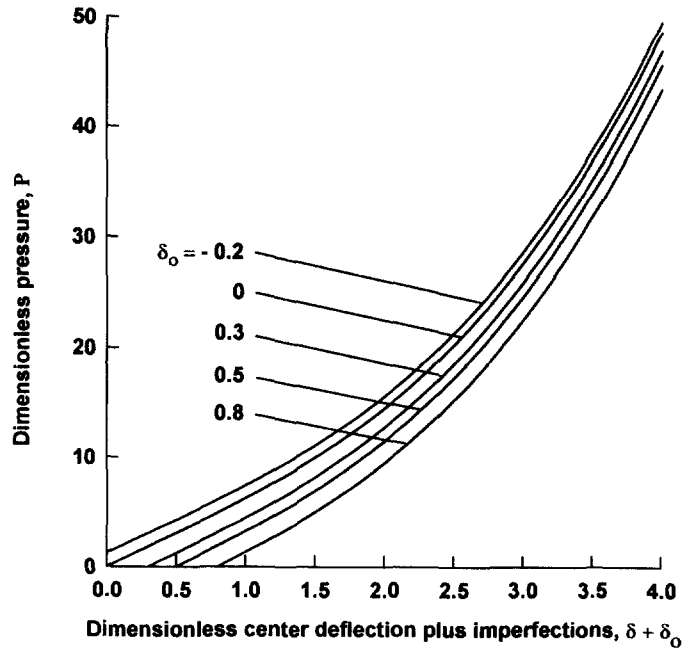

Fig. 1. Influence of initial geometric imperfection on the pressure–deflection interaction of a spherical cap ($L/R_1 = L/R_2 = 0.5$). Movable edges.

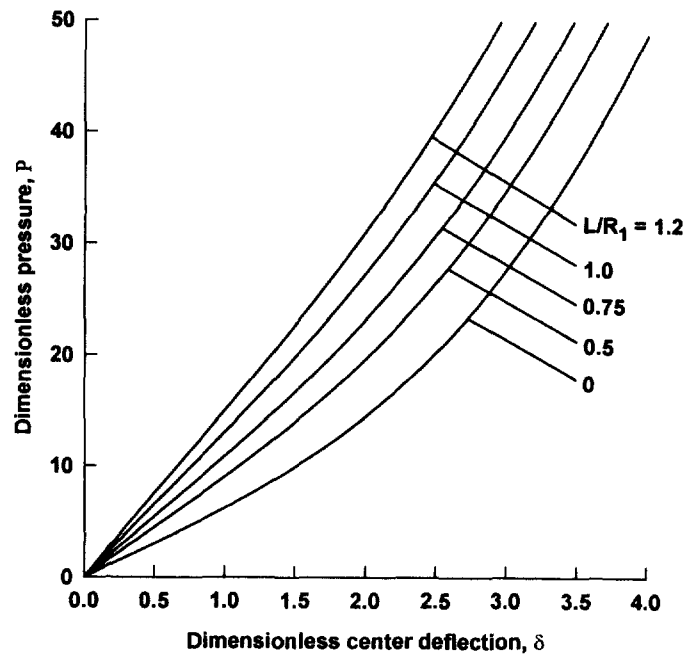

Fig. 2. Influence of the curvature ratio of a geometrically perfect doubly-curved panel ($L/R_2 = 1$) on the pressure–deflection interaction. Movable edges.

movable and immovable edges is displayed. The response behavior as appearing from these figures reveals a net departure from that featured by the standard laminated structure counterpart. In contrast to the latter case, in the former one the total absence of the snapping phenomenon can be remarked. In the case of standard laminated structures, such a trend is proper to flat panels only.

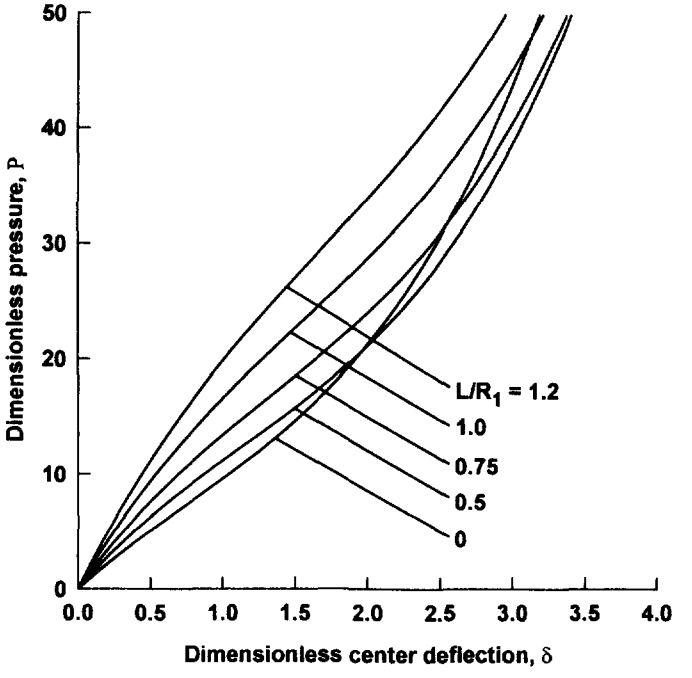

Fig. 3. Counterpart of Fig. 2. The four edges are immovable.

The beneficial influence of negative imperfections on the loading carrying capacity of panels emerges from Fig. 1. Figures 2 and 3 reveal the effects played by the curvature and edge movability/immovability on the load carrying capacity of panels. The results reveal that in contrast to the case of panels with all edges movable, the immovability of the edges provides an increase of their load bearing capacity. In addition, the results reveal that in the latter case, the load carrying capacity of the panel becomes less sensitive to the change of the curvature L/R_1 than in the case of the movable edge panel counterpart. Figure 4 depicts the response of a uniaxial-compressed circular cylindrical panel. In addition to the case of the geometrically perfect panel, a number of scenarios consisting of various combinations of the lateral pressure and initial geometric imperfections are considered in this figure. A sketch of a circular cylindrical sandwich panel is provided in the inset of the figure.

The results emphasize the equivalent role, from the response standpoint, played by the initial geometric imperfection and a lateral pressure. The similarity in the response behavior with a flat laminated composite panel becomes also evident from this figure.

In Figs 5 and 6 the effect of the geometric initial imperfection on the response of a spherical cap subjected to the uniaxially compression rise is presented. The results emerging from the graphs reveal that corresponding to $\delta_0 = 0.2566$, the panel exhibits buckling bifurcation while, for any $\delta_0 \neq 0.2566$, a monotonous increase of the deflection amplitude with that of the compressive load is experienced. The absence of the snapping phenomenon, as well as the similarity, as concerns the postbuckling behavior, with a flat panel becomes also apparent from these plots. This behavior constitutes a noteworthy departure from that featured by the standard laminated or homogeneous shell counterpart whose load carrying capacity is strongly affected by the emergence of the snap-through phenomenon and is imperfection-sensitive (see e.g. Librescu and Chang, 1992; Librescu *et al.*, 1993).

In Figs 7 and 8 the response of a doubly-curved panel of $K \gtrless 0$, subjected to the uniaxially compression rise is depicted, where $K(\equiv 1/(R_1, R_2))$ denotes the Gaussian curvature. The results show that for specific values of the principal curvatures (in this case for $L/R_2 = 0.5$ and $L/R_1 = -0.15$) a buckling bifurcation is experienced. For the same cases, following the increase of the compressive edge load beyond the buckling bifurcation, a snap-through buckling is manifested. Based on these results one can conclude that for

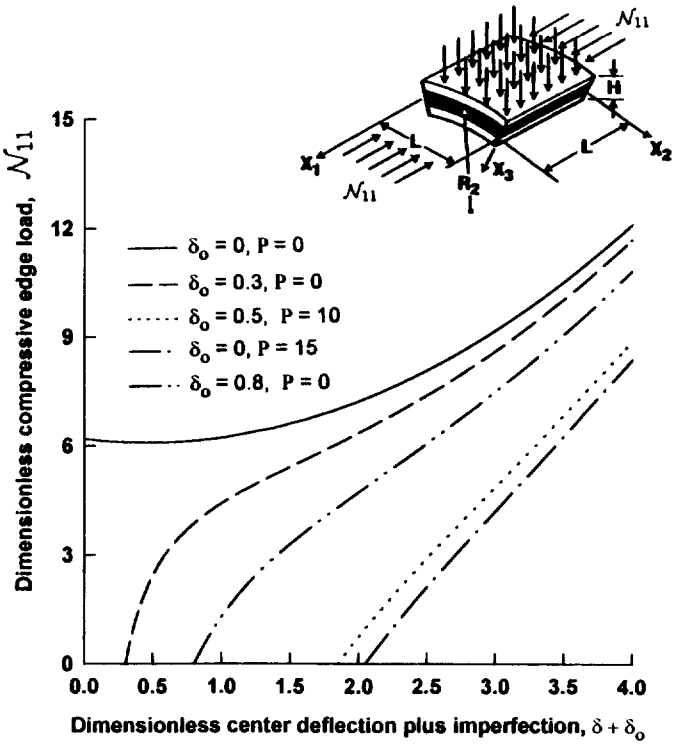

Fig. 4. Influence of combinations of the pressure and initial geometric imperfections on the compressive load–deflection interaction of a circular cylindrical panel ($L/R_1 = 0$, $L/R_2 = 1$). Movable edges.

sandwich structures, the ones featuring a negative Gaussian curvature are more prone to the snapping phenomenon than their counterparts featuring a positive Gaussian curvature.

The same trend is also highlighted in Figs 9 and 10 where the considered structures feature negative Gaussian curvatures. From these plots it becomes apparent that for the same structure, for a specific pressure (Fig. 9), and a geometric imperfection amplitude (Fig. 10) one gets a buckling bifurcation, followed, with the increase of the compressive edge load, by the snapping phenomenon. Based on these findings one can conclude that for a panel of given negative Gaussian curvature there is a single pressure and geometric imperfection, or combination of both, for which buckling bifurcation, followed by the snapping phenomenon can occur. However, as Fig. 11 reveals, a sandwich circular cylindrical shell can also experience a mild snap-through buckling. A similar conclusion was conjectured by Fulton (1961).

In Figures 12 and 13 the case of a geometrically-perfect doubly-curved panel featuring positive and negative Gaussian curvatures is considered. One assumes that the panel belongs to the Type (ii) and is subjected to the uniaxially compressive edge load rise. The figures show that the increase of the orthotropy ratio of the faces (measured in terms of the ratio E_1/E_2), yields an increase of the load carrying capacity of the panel. Compared with the panel counterpart featuring freely movable edges, the results (not displayed here), reveal that in the case of immovable edges the panel displays an increased load carrying capacity.

Moreover, a comparison with the results displayed in Fig. 7 where the faces are characterized by $E_1/E_2 = 1$, and where for $L/R_1 = -0.15$, a snap-through buckling occurs, in the present case, due to the relative large orthotropy ratio, an inhibition of the intensity of the snapping phenomenon is manifested.

It should also be stressed that in the case of immovable edges, in addition to the primary branches, also secondary branches can occur. In the experimental work, a snap-through from the primary to the secondary branches can be experienced. Such a trend was illustrated in the inset of Fig. 14. Although the circular cylindrical panel features the largest

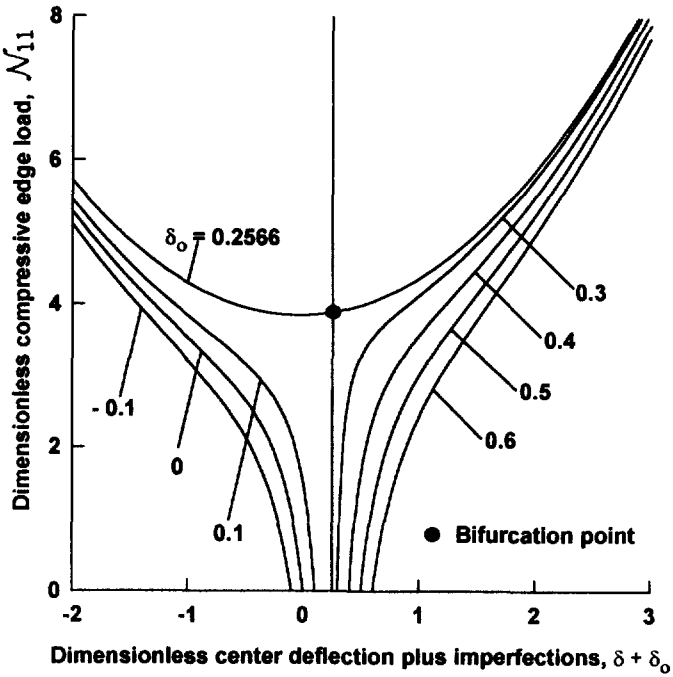

Fig. 5. Influence of the initial geometric imperfection on the compressive load–deflection interaction of a spherical cap ($L/R_1 = L/R_2 = 0.1$). Movable edges.

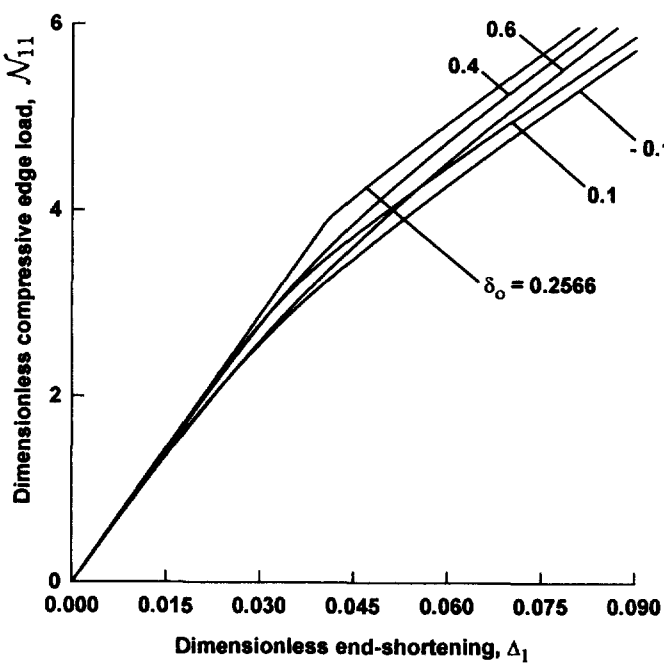

Fig. 6. Counterpart of Fig. 5 in the ($\mathcal{N}_{11}, \Delta_1$) plane.

load carrying capacity, the snap-through from the first to the second branches can occur, in this case, at the lowest possible compressive edge load.

Although in this paper the equations incorporate also the dynamical effects, only the statistical counterpart of these equations have been used. In spite of this, the full dynamical equations enable one to study a problem of high importance, namely that of frequency-load interaction. Such a study can be done along the lines pursued in a number of relevant papers (see e.g. Librescu and Chang, 1992, 1993).

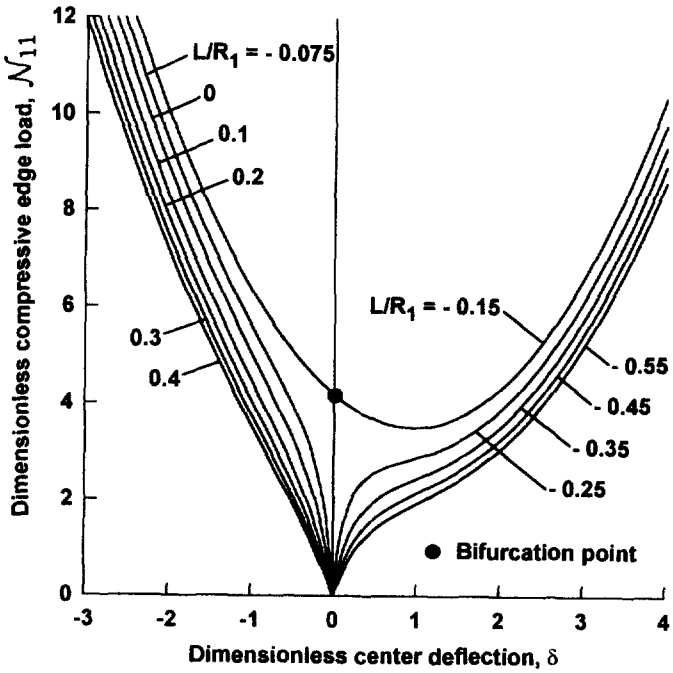

Fig. 7. Influence of the curvature on the compressive load–deflection interaction of doubly-curved ($L/R_2 = 0.5$) panel. Two edges are immovable.

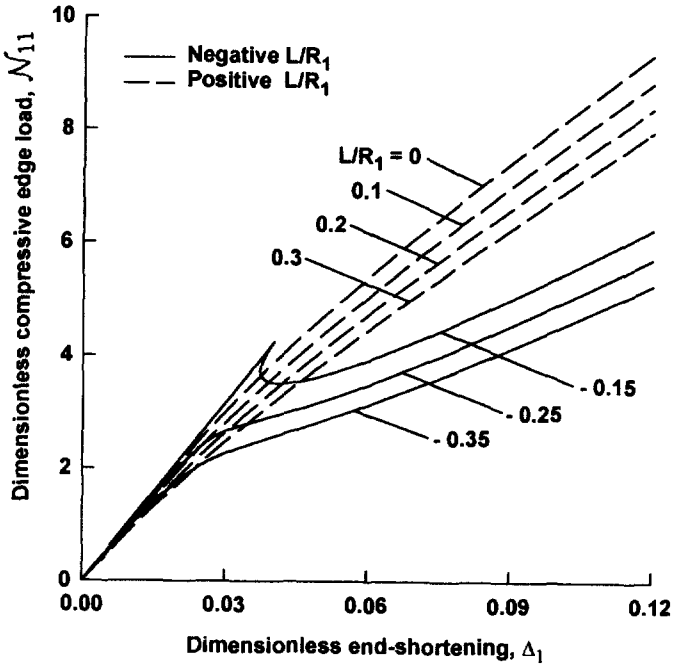

Fig. 8. Counterpart of Fig. 7 in the plane ($\mathcal{N}_{11}, \Delta_1$).

9. CONCLUSIONS

A number of issues related to the postbuckling of flat and curved sandwich panels have been examined and pertinent conclusions about the influence played in this respect by a number of kinematical and physical parameters have been outlined. As an important outcome of this study, the low intensity and even the absence, of both the snapping phenomenon and sensitivity to initial geometric imperfections of the load carrying capacity

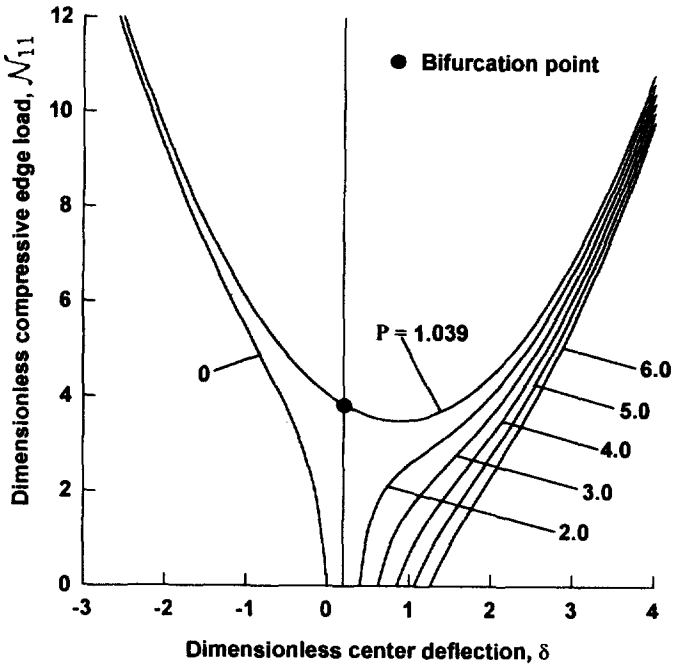

Fig. 9. Influence of a lateral pre-load on the compressive load–deflection interaction of a doubly curved panel ($L/R_1 = -0.05$, $L/R_2 = 0.5$). Two edges are immovable.

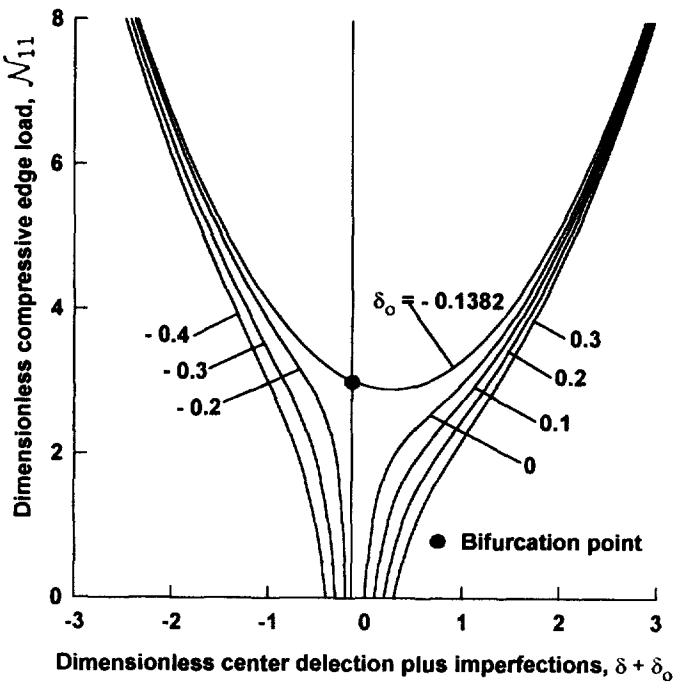

Fig. 10. Influence of the initial geometric imperfection on the compressive load–deflection interaction of a doubly curved panel ($L/R_1 = -0.1$; $L/R_2 = 0.1$). Two edges are immovable.

of curved sandwich panels was revealed. It was also shown that in some very special instances (e.g., of panels feature negative Gaussian curvatures), the snapping has a larger probability to occur. The strong influence on the enhancement of the load carrying capacity of panels played by the immovability of edges and the increase of the orthotropicity ratio of facings was also highlighted.

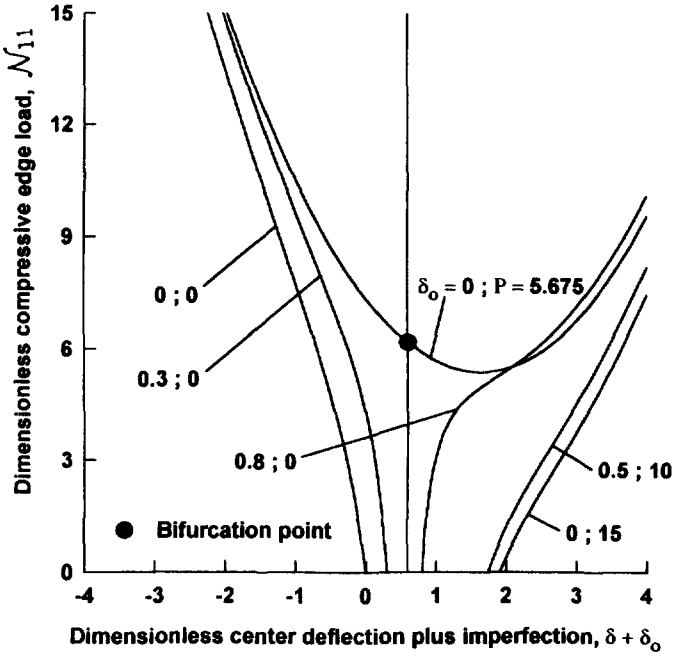

Fig. 11. Influence of combined initial geometric imperfections on lateral pre-load on the compressive load–deflection interaction of a circular cylindrical panel ($L/R_1 = 0$, $L/R_2 = 1$). Two edges are immovable.

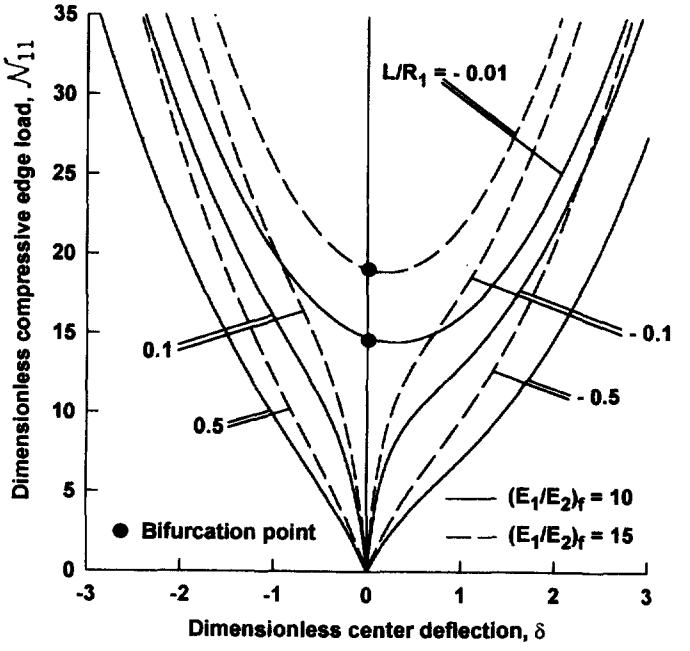

Fig. 12. Influence of the curvature and orthotropicity ratio of faces on the compressive load–deflection interaction of doubly-curved ($L/R_2 = 0.5$) panels. Two edges are immovable. Panel of Type (ii).

It is hoped that the results of this study will contribute to a better understanding and design of sandwich structures subjected to complex loading conditions.

Acknowledgement—The work reported herein was supported by NASA Langley Research Center under Grant NAG 1-1689.

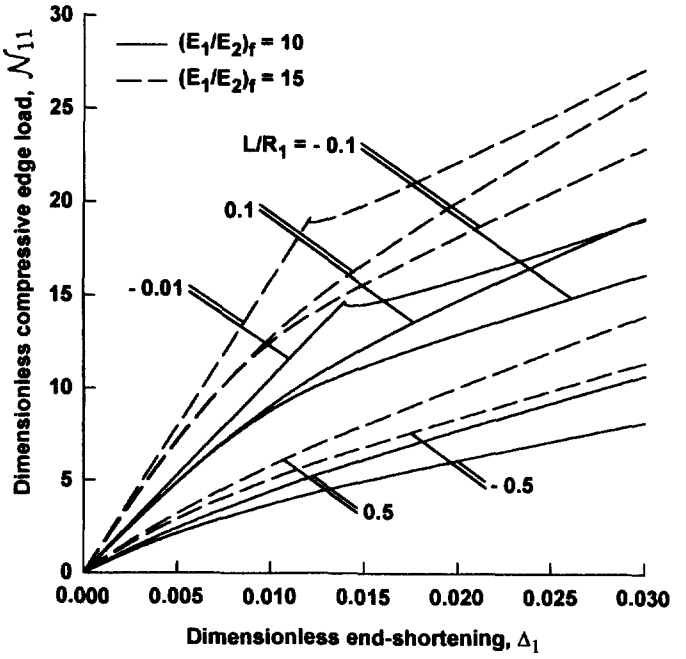

Fig. 13. Counterparts of Fig. 12 in the plane $(\mathcal{N}_{11}, \Delta_1)$.

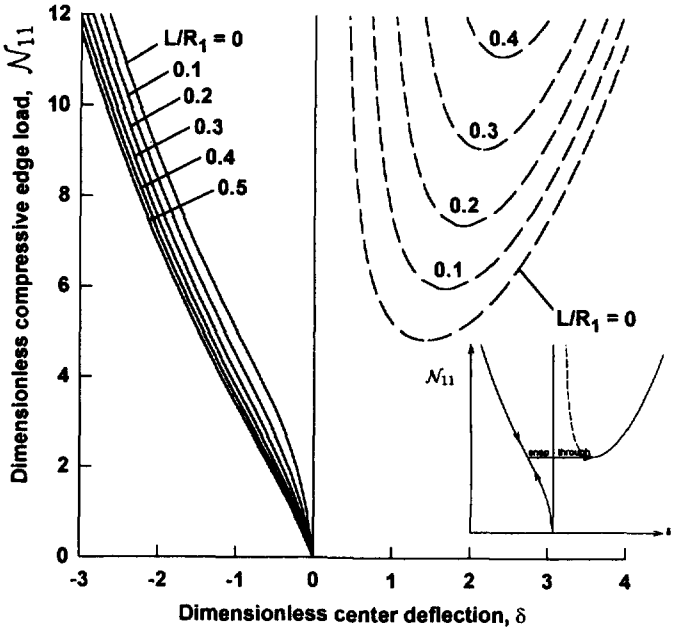

Fig. 14. Primary and secondary paths in a doubly-curved ($L/R_2 = 0.5$) panel. The inset highlights the possibility of the snap-through occurrence.

REFERENCES

Arbocz, J. (1997) Future directions and challenges in shell stability analysis. *Proceedings of the 38th AIAA/ASME/ASCE/AHS/ASC Structures, Structural Dynamics, Materials Conference and Exhibition and AIAA/ASME/AHS/Adaptive Structures Forum*, Paper AIAA-97-1077, pp. 1949–1959, Kissimmee, Florida, April, 1997.

Bushnell, D. (1985) *Computerized Buckling Analysis of Shells*. Martinus Nijhoff, Dordrecht/Boston/Lancaster.

Fulton, R. E. (1961) Non-linear equations for a shallow unsymmetric sandwich shell of double curvature. *Developments in Mechanics, Proceedings of 7th Midwestern Mechanical Conference*. Plenum Press, New York, N.Y., pp. 365–380.

Karavanov, V. F. (1960) Stability of three-layer shallow cylindrical panels with soft core. *Izvestia Vishish Ukebnich Zavedenia-Aviatsionaia Technika* **2**, 50–60 (in Russian).

Librescu, L. (1965) Aeroelastic stability of orthotropic heterogeneous thin panels in the vicinity of the flutter critical panel. 4, *Journal de Mécanique*, 4 **1**, 51–76.
Librescu, L. (1975) *Elastostatics and Kinetics of Anisotropic and Heterogeneous Shell-Type Structures*, Chapters V–VII, pp. 493–540. Noordhoff International Publishers, Leyden, The Netherlands.
Librescu, L. (1987) Refined geometrically non-linear theories of anisotropic laminated shells. *Quarterly of Applied Mathematics* **45**(1), 1–22.
Librescu, L. and Chang, M. Y. (1992) Post-buckling and imperfection sensitivity of shear deformable composite doubly-curved panels. *International Journal of Solids and Structures* **29**(9), 1065–1083.
Librescu, L. and Chang, M. Y. (1992) Vibration of compressively loaded shear deformable flat panels exhibiting initial geometric imperfections. *AIAA Journal* **30**(11), 2793–2795.
Librescu, L. and Chang, M. Y. (1993) Effects of geometric imperfections on vibration of compressed shear deformable laminated composite curved panels. *Acta Mechanica* **96**, 203–224.
Librescu, L., Lin, W., Nemeth, M. P. and Starnes, J. H., Jr. (1995) Thermomechanical post-buckling of geometrically imperfect flat and curved panels taking into account tangential edge constraints. *Journal of Thermal Stresses* **18**(4), 465–482.
Librescu, L., Lin, W., Nemeth, M. P. and Starnes, J. H., Jr. (1993) Classical vs non-classical postbuckling behavior of laminated composite panels under complex loading conditions. *Non-Classical Problems of the Theory and Behavior of Structures Exposed to Complex Environmental Conditions*, AMD-Vol. 165, ASME, Ed. L. Librescu, pp. 169–182.
Librescu, L., Hause, T. and Camarda, C. J. (1996) Geometrically nonlinear models of initially imperfect anisotropic sandwich plates and shells incorporating non-classical effects. *Proceedings of the 37th AIAA/ASME/ASCE/AHS/ASC Structures, Structural Dynamics and Materials Conference and Exhibit*, Paper AIAA-96-1350, Part 1, pp. 284–299, Salt Lake City, UT, 15–17 April 1996.
Noor, A. K., Burton, W. S. and Bert, C. W. (1966) Computational models for sandwich panels and shells. *Applied Mechanics Reviews* **4**(3), 155–199.
Seide, P. (1974) A re-examination of Koiter's theory of initial postbuckling behavior and imperfection sensitivity of structures. *Thin Shell Structures: Theory, Experimental and Design*, Ed. C. Y. Fung and E. E. Sechler, pp. 59–80. Prentice-Hall, New Jersey.
Simitses, G. J. (1986) Buckling and postbuckling of imperfect cylindrical shells: a review. *Applied Mechanics Reviews* **39**(10), 1517–1524.

APPENDIX 1

Strain–Displacement Relationships

Bottom Facings

$$
\begin{aligned}
{}'\varepsilon_{11} &= \xi_{1,1}+\eta_{1,1}+\tfrac{1}{2}v_{3,1}^2+v_{3,1}\mathring{v}_{3,1}-v_3/R_1 \quad (1 \rightleftarrows 2)\\
{}'\gamma_{12} &= \xi_{1,2}+\xi_{2,1}+\eta_{1,2}+\eta_{2,1}+v_{3,1}v_{3,2}+\mathring{v}_{3,1}v_{3,2}+v_{3,1}\mathring{v}_{3,2}\\
{}'\kappa_{11} &= -v_{3,11} \quad (1 \leftrightarrows 2)\\
{}'\kappa_{12} &= -2v_{3,12}.
\end{aligned}
$$

Core Layer

$$
\begin{aligned}
\bar{\varepsilon}_{11} &= \xi_{1,1}+\tfrac{1}{2}v_{3,1}^2+\mathring{v}_{3,1}v_{3,1}-v_3/R_1 \quad (1 \leftrightarrows 2)\\
\bar{\gamma}_{12} &= \xi_{1,2}+\xi_{2,1}+v_{3,1}v_{3,2}+\mathring{v}_{3,1}v_{3,2}+v_{3,1}\mathring{v}_{3,2}\\
\bar{\kappa}_{11} &= \frac{1}{\bar{h}}\left\{\eta_{1,1}+\frac{1}{2}hv_{3,11}\right\} \quad (1 \leftrightarrows 2)\\
\bar{\kappa}_{12} &= \frac{1}{\bar{h}}\{\eta_{1,2}+\eta_{2,1}hv_{3,12}\}\\
\bar{\gamma}_{13} &= \frac{1}{\bar{h}}\left\{\eta_1+\frac{1}{2}hv_{3,1}\right\}+v_{3,1} \quad (1 \leftrightarrows 2).
\end{aligned}
$$

Top Facings

$$
\begin{aligned}
{}''\varepsilon_{11} &= \xi_{1,1}-\eta_{1,1}+\tfrac{1}{2}(v_{3,1})^2+\mathring{v}_{3,1}v_{3,1}-v_3/R_1 \quad (1 \leftrightarrows 2)\\
{}''\gamma_{12} &= \xi_{1,2}+\xi_{2,1}-\eta_{1,2}-\eta_{2,1}+v_{3,1}v_{3,2}+\mathring{v}_{3,1}v_{3,2}+v_{3,1}\mathring{v}_{3,2}\\
{}''\kappa_{11} &= -v_{3,11} \quad (1 \leftrightarrows 2)\\
{}''\kappa_{12} &= -2v_{3,12}.
\end{aligned}
$$

APPENDIX 2

Expressions of the coefficients appearing in eqns (31), (32), (34) and (36)

$$\tilde{A}_1 = \frac{(A_{11}A_{22} - A_{12}^2)\mu_n^2}{32A_{11}\lambda_m^2}$$

$$\tilde{A}_2 = \frac{(A_{11}A_{22} - A_{12}^2)\lambda_m^2}{32A_{22}\mu_n^2}$$

$$\tilde{A}_3 = \frac{(\mu_n^2/R_1 + \lambda_m^2/R_2)(A_{11}A_{22}A_{66} - A_{66}A_{12}^2)}{\tilde{\Delta}_{mn}}$$

$$\tilde{B}_1 = \frac{a\{[(A_{12} + A_{66})d_2 - A_{22}d_1]\lambda_m\mu_n^2 - d_1A_{66}\lambda_m^3 - d_1d_2\lambda_m\}}{\hat{\tilde{\Delta}}_{mn}}$$

$$\tilde{C}_1 = \frac{a\{[(A_{12} + A_{66})d_1 - A_{11}d_2]\lambda_m^2\mu_n - d_2A_{66}\mu_m^3 - d_1d_2\mu_m\}}{\hat{\tilde{\Delta}}_{mn}}$$

$$\tilde{D}_1 = \frac{-\lambda_m^2}{8}, \quad \tilde{D}_2 = \frac{A_{12}\mu_n^2 - A_{11}\lambda_m^2}{16A_{11}\lambda_m}, \quad d_1 = \frac{2\bar{K}^2\bar{G}_{13}}{\bar{h}}, \quad d_2 = \frac{2\bar{K}^2\bar{G}_{23}}{\bar{h}}$$

$$\tilde{D}_4 = \frac{(A_{12}A_{66} + A_{12}^2 - A_{11}A_{22})\lambda_m\mu_n^2 - A_{11}A_{66}\lambda_m^3}{R_1\,\tilde{\Delta}_{mn}} + \frac{A_{22}A_{66}\lambda_m\mu_n^2 - A_{12}A_{66}\lambda_m^3}{R_2\,\hat{\Delta}_{mn}}$$

$$D_5 = \frac{-A_{22}}{A_{11}A_{22} - A_{12}^2}, \quad D_6 = \frac{A_{12}}{A_{11}A_{22} - A_{12}^2}, \quad \tilde{E}_1 = \frac{-\mu_n^2}{8}, \quad \tilde{E}_2 = \frac{A_{12}\lambda_m^2 - A_{22}\mu_n^2}{16A_{22}\mu_n}, \quad \tilde{E}_3 = \frac{\mu_n}{16}$$

$$\tilde{E}_4 = \frac{A_{12}A_{66} + A_{12}^2 - A_{11}A_{22}\lambda_m^2\mu_n - A_{22}A_{66}\mu_n^3}{R_2\,\hat{\Delta}_{mn}} + \frac{A_{11}A_{66}\lambda_m^2\mu_n - A_{12}A_{66}\mu_n^3}{R_1\,\hat{\Delta}_{mn}}$$

$$E_5 = \frac{A_{12}}{A_{11}A_{22} - A_{12}^2}, \quad E_6 = \frac{-A_{11}}{A_{11}A_{22} - A_{12}^2}.$$

In these expressions, $\hat{\Delta}_{mn}$ and $\hat{\tilde{\Delta}}_{mn}$ are defined as follows:

$$\hat{\Delta}_{mn} = A_{11}A_{66}\lambda_m^4 + (A_{11}A_{22} - 2A_{12}A_{66} - A_{12}^2)\lambda_m^2\mu_n^2 + A_{22}A_{66}\mu_n^4$$

$$\hat{\tilde{\Delta}}_{mn} = A_{11}A_{66}\lambda_m^4 + (d_2A_{11} + d_1A_{66})\lambda_m^2 + (A_{11}A_{22} - 2A_{12}A_{66} - A_{12}^2A_{66} - A_{12}^2)\lambda_m^2\mu_n^2 + (d_1A_{22} + d_2A_{66})\mu_n^2 + A_{22}A_{66}\mu_n^2 + A_{22}A_{66}\mu_n^4 + d_1d_2.$$